Structural investigations of β-CaAlF$_5$ by coupling powder XRD, NMR, EPR and spectroscopic parameter calculations

M. Body[a,b,*], G. Silly[c], C. Legein[b], J.-Y. Buzaré[a], F. Calvayrac[a], P. Blaha[d]

[a]*Laboratoire de Physique de l'Etat Condensé, CNRS UMR 6087, Institut de Recherche en Ingénierie Moléculaire et Matériaux fonctionnels, CNRS FR 2575, Université du Maine, Avenue Olivier Messiaen, 72085 Le Mans Cedex 9, France*
[b]*Laboratoire des Oxydes et Fluorures, CNRS UMR 6010, Institut de Recherche en Ingénierie Moléculaire et Matériaux fonctionnels, CNRS FR 2575, Université du Maine, Avenue Olivier Messiaen, 72085 Le Mans Cedex 9, France*
[c]*Laboratoire de Physicochimie de la Matière Condensée, CNRS UMR 5617, Institut Charles Gerhardt, CNRS FR 1878, Université de Montpellier II, Place Eugène Bataillon, C.C. 03, 34095 Montpellier Cedex 5, France*
[d]*Institute of Materials Chemistry, Vienna University of Technology, A-1060 Vienna, Getreidemarkt 9/165-TC, Austria*

Abstract

β-CaAlF$_5$ was synthesized by solid-state reaction. The precise structure was refined from X-ray powder diffraction data in the monoclinic space group $P2_1/c$ with lattice constants $a = 5.3361$ Å, $b = 9.8298$ Å, $c = 7.3271$ Å, and $\beta = 109.91°$ ($Z = 4$). The structure exhibits isolated chains of AlF$_6^{3-}$ octahedra sharing opposite corners. ^{19}F and ^{27}Al solid state NMR spectra were recorded using MAS and SATRAS techniques. An EPR spectrum was recorded for β-CaAlF$_5$:Cr^{3+}. The experimental spectra were simulated in order to extract the NMR and EPR parameter values. Five fluorine sites and one low symmetry aluminium site were found in agreement with the refined structure.

These parameters were calculated using empirical and ab-initio methods. The agreement obtained between the calculated ^{19}F chemical shift values, ^{27}Al quadrupolar parameters, Cr^{3+} EPR fine structure parameters and the experimental results demonstrates the complementarity of XRD, magnetic resonance experiments and theoretical methodologies.
© 2005 Elsevier Inc. All rights reserved.

1. Introduction

The solid–liquid phase diagram of the binary system CaF$_2$–AlF$_3$ shows two compounds: dimorphic CaAlF$_5$ with a reversible transition $\alpha \leftrightarrow \beta$ around 740 °C, and Ca$_2$AlF$_7$ [1,2]. β-CaAlF$_5$ is the high temperature phase and was first identified by Holm in 1965 [3]. Ravez et al. found that this phase was isotypic with CaFeF$_5$, and determined its cell parameters in the orthorhombic crystal system [4]. A determination of CaFeF$_5$ structure was achieved in the monoclinic $P2_1/c$ space group by Von der Mühll et al. in 1974, and new cell parameters were also determined for β-CaAlF$_5$ in this space group [5]. Then a refinement of the CaFeF$_5$ structure has been recently performed by Graulich et al. [6] leading to less distorted FeF$_6^{3-}$ octahedra.

The first aim of the study is to determine the precise structure of β-CaAlF$_5$ using X-ray powder diffraction method and to investigate local order with magnetic resonance spectrocopies (^{19}F, ^{27}Al NMR and Cr^{3+} EPR). The second one is to apply empirical or ab-initio calculation methods of the NMR and EPR parameters and to compare the experimental and calculated values to support the structure determination.

It will be shown that such a study is a good example of the complementarity between X-ray powder diffraction, magnetic resonance techniques and theoretical methodologies.

*Corresponding author. Laboratoire de Physique de l'Etat Condensé, CNRS UMR 6087, Institut de Recherche en Ingénierie Moléculaire et Matériaux fonctionnels, CNRS FR 2575, Université du Maine, Avenue Olivier Messiaen, 72085 Le Mans Cedex 9, France. Fax: +33 2 43 83 35 06.

E-mail address: monique.body@univ-lemans.fr (M. Body).

2. Experimental section

2.1. Sample preparation

Owing to the fact that fluoride compounds are moisture sensitive, all preparative works (weighting, mixing and grinding) were done inside a dry glove box. As outlined in Ref. [4], α and β-CaAlF$_5$ may be both prepared by solid-state reaction after quenching, with heating temperatures equal to 700 and 840 °C respectively. For our part, we obtain a white powder of β-CaAlF$_5$ by solid state reaction [7]: after preliminary mixing, the stoichiometric mixture of CaF$_2$ (from CERAC) and AlF$_3$ (from ASTRON) was heated at 850 °C during 96 h in sealed platinum tubes and then quenched in water. The same synthesis protocol was used for doped β-CaAlF$_5$:Cr^{3+} (CaF$_2$, 0.99 AlF$_3$, 0.01 CrF$_3$). The purity of the obtained phases was controlled by X-ray diffraction powder method. In agreement with data entries in the Powder Diffraction File numbers 20-0196, 80-1728 for α-CaAlF$_5$ and 20-0197 for β-CaAlF$_5$, and despite the poor quality of the 20-0196 and 20-0197 files, a pure β phase could be identified in our samples.

2.2. X-ray powder diffraction

The powder X-ray diffraction pattern was recorded at room temperature with a Philips X'pert PRO diffractometer, equipped with an X'celerator detector. Measurements were done in the 2θ range from 15° to 135° using Cu$K\alpha_{1,2}$ X-rays with an interpolated step of 0.017°, during 144 min. The Rietveld method [8] using the Fullprof [9] program was used for the structural refinement.

2.3. NMR

^{19}F MAS NMR spectra were recorded at 705.7 MHz on a Bruker Avance 750 spectrometer using a high speed CP MAS probe with a 2.5 mm rotor spinning at $v_r = 34$ kHz. The external reference chosen for ^{19}F isotropic chemical shift determination is C$_6$F$_6$ (δ(C$_6$F$_6$) vs. CFCl$_3$ = -164.2 ppm) [10]. Reconstructions of the ^{19}F NMR spectra were performed with DMFIT software [11], including spinning sidebands, using six adjustable parameters: isotropic chemical shift δ_{iso}, chemical shift anisotropy δ_{aniso}, chemical shift asymmetry parameter η_{CS}, line width, relative line intensity and line shape. δ_{iso}, δ_{aniso}, η, the relative line intensity and the line shape were assumed to be independent of the spinning rate.

The ^{27}Al SATRAS NMR spectrum was recorded at 78.2 MHz on a Bruker Avance 300 spectrometer using a high speed CP MAS probe with a 2.5 mm rotor spinning at $v_r = 25$ kHz. 1 M solution of Al(NO$_3$)$_3$ was used as an external reference for ^{27}Al chemical shift. The reconstruction of this spectrum was achieved using a homemade FORTRAN 95 code based on the theoretical treatment of SATRAS NMR spectra developed by Skibsted et al. [12,13]. A few errors in the original formula of [12] have

been corrected in [14,15]. The measured parameters are the quadrupolar frequency v_Q, the asymmetric parameter η_Q, and the chemical shift tensor δ.

2.4. EPR

In aluminates, the Cr^{3+} ion which substitutes for Al^{3+} is often used as an EPR local probe. The EPR X-band (9.817 GHz) spectrum was recorded on a Bruker spectrometer at room temperature. The relevant spin-Hamiltonian for Cr^{3+} ($S = \frac{3}{2}$) in a powder sample is

$$H = \mu_B \vec{H} \cdot \tilde{g} \cdot \vec{S} + \frac{1}{3}(b_2^0 O_2^0 + b_2^2 O_2^2)$$
$$= \mu_B \vec{H} \cdot \tilde{g} \cdot \vec{S} + \frac{1}{3} b_2^0 (O_2^0 + \lambda O_2^2),$$

where the first term is the electronic Zeeman interaction and the second one is the fine-structure or zero field splitting (ZFS) term. The O$_n^m$ are the well-known Stevens spin operators and $\lambda = b_2^2/b_2^0$ is the asymmetry parameter.

The EPR spectrum was calculated using a code [16] called EPR-ULM in [17]. In this code the line width anisotropy is taken into account and interpreted in terms of broadening effects due to site-to-site distributions of the fine structure parameters and treated using first-order perturbation theory. It is possible to take into account small distributions of any fine structure parameter. The distribution of each parameter is characterized by a small perturbation quantity δb_2^m, which may be seen as half the width of the corresponding b_2^m parameter distribution. All the other broadening effects, such as the natural linewidth, and the dipolar and hyperfine broadenings, are modelled by a constant linewidth Γ_0.

3. Results

3.1. Crystal structure determination

According to Ravez et al. [4], β-CaAlF$_5$ is isotypic with CaFeF$_5$ which crystallizes in the monoclinic space group $P2_1/c$. This solution was tested and almost all the peaks of the diffraction pattern could be indexed using this space group (a very small amount of AlF$_3$ was detected which was not taken into account in the refinement). The cell parameters are $a = 5.3361(1)$ Å, $b = 9.8298(2)$ Å, $c = 7.3271(1)$ Å, and $\beta = 109.911(1)°$ ($Z = 4$). The cell volume is equal to 361.35 Å^3, and is smaller than the cell volume of CaFeF$_5$, which is equal to 395.10 Å^3 [6], owing to the fact that the Al^{3+} ion is smaller than the Fe^{3+} ion.

Then, the atomic coordinates of CaFeF$_5$ determined in [5] were used as starting data in a Rietveld refinement after replacing the Fe atoms ions by Al atoms. The final Rietveld X-ray data analysis is shown in Fig. 1. The last cycle of the least square refinement contained terms for 42 parameters and converged to agreement factors $R_{Bragg} = 0.0571$, $R_P = 0.106$, $R_{wp} = 0.0965$, $\chi^2 = 0.0579$ and $R_{exp} = 0.0402$. The atomic coordinates and isotropic temperature factors
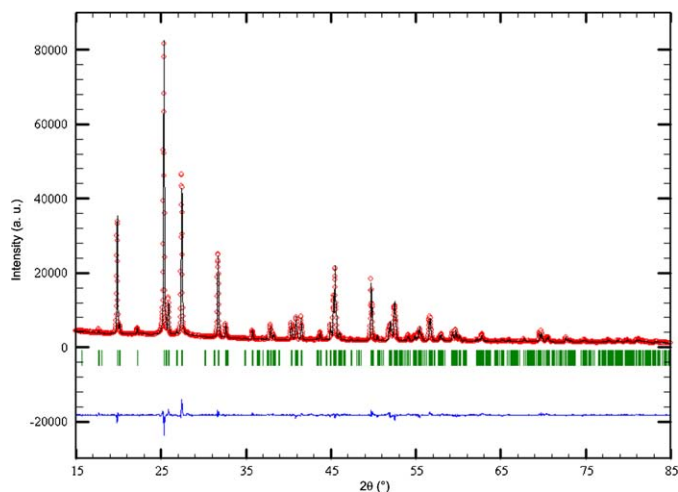
Fig. 1. Observed (points) and calculated (line) powder X-ray diffraction patterns of β-CaAlF$_5$. The difference pattern is shown below at the same scale, the vertical bars are related to the calculated Bragg reflection positions.

Table 1
Powder X-ray refined fractional atomic coordinates and thermal parameters, and WIEN2k optimized fractional atomic coordinates (in italic) for β-CaAlF$_5$

Atoms	Site	x	y	z	B_{iso} (Å^2)
Ca	4e	0.4717(4)	0.4818(2)	0.2460(4)	2.9(1)
		0.4709	*0.4808*	*0.2438*	
Al	4e	0.0985(5)	0.2502(4)	−0.1001(6)	2.1(1)
		0.1059	*0.2524*	*0.8996*	
F(1)	4e	0.1081(8)	0.6104(5)	0.1751(8)	3.4(1)
		0.1150	*0.6097*	*0.1798*	
F(2)	4e	0.8468(9)	0.3632(4)	0.3541(8)	2.3(1)
		0.8416	*0.3635*	*0.3545*	
F(3)	4e	0.6273(8)	0.6277(4)	0.0603(8)	3.7(2)
		0.6178	*0.6255*	*0.0540*	
F(4)	4e	0.1473(6)	0.2812(4)	0.1574(9)	2.7(1)
		0.1384	*0.2841*	*0.1583*	
F(5)	4e	0.3368(8)	0.1207(4)	0.9849(9)	3.0(1)
		0.3502	*0.1167*	*0.9884*	

Table 2
Selected bond distances and angles as deduced from powder X-ray structure refinement and WIEN2k optimization (in italic) for β-CaAlF$_5$

Bond distances (Å)

Ca–F(2)	2.217(5)	Al–F(2)	1.689(5)
	2.193		*1.755*
Ca–F(1)	2.224(5)	Al–F(1)	1.727(5)
	2.197		*1.760*
Ca–F(3)	2.317(8)	Al–F(5)	1.757(5)
	2.305		*1.823*
Ca–F(5)	2.329(7)	Al–F(3)	1.837(5)
	2.296		*1.841*
Ca–F(5)	2.336(9)	Al–F(4)	1.840(8)
	2.309		*1.869*
Ca–F(3)	2.380(8)	Al–F(4)	1.907(8)
	2.318		*1.870*
Ca–F(4)	2.558(5)		
	2.554		

Bond angles (°)

F(2)–Al–F(1)	94.7(3)	F(1)–Al–F(4)	96.1(3)
	91.9		*95.9*
F(2)–Al–F(5)	91.3(3)	F(5)–Al–F(3)	88.6(3)
	91.3		*88.9*
F(2)–Al–F(3)	177.7(3)	F(5)–Al–F(4)	85.6(3)
	179.7		*84.9*
F(2)–Al–F(4)	98.0(3)	F(5)–Al–F(4)	84.3(3)
	95.2		*87.2*
F(2)–Al–F(4)	93.4(3)	F(3)–Al–F(4)	84.4(3)
	91.4		*88.5*
F(1)–Al–F(5)	173.9(3)	F(3)–Al–F(4)	84.2(3)
	176.7		*85.0*
F(1)–Al–F(3)	85.4(2)	F(4)–Al–F(4)	165.0(3)
	87.9		*169.9*
F(1)–Al–F(4)	92.7(3)	Al–F(4)–Al	155.8(4)
	91.6		*157.0*

are listed in Table 1. β-CaAlF$_5$ exhibits five sites for fluorine and one for calcium and aluminium. Selected characteristic inter-atomic distances and angles are given in Table 2.

3.2. Crystal structure description

The crystal structure of β-CaAlF$_5$ and α-CaAlF$_5$ present several common features. Effectively, β-CaAlF$_5$, like CaFeF$_5$ [6], and α-CaAlF$_5$ [18] are built up from isolated infinite chains of M^{III}F$_6^{3-}$ octahedra along the *c*-axis, as shown in Fig. 2. The M^{III}F$_6^{3-}$ octahedra share opposite corners. These octahedra are distorted and the longest M^{III}–F distance involves the F4 shared atoms. The chains are corrugated and the M^{III}–F–M^{III} angle is equal to
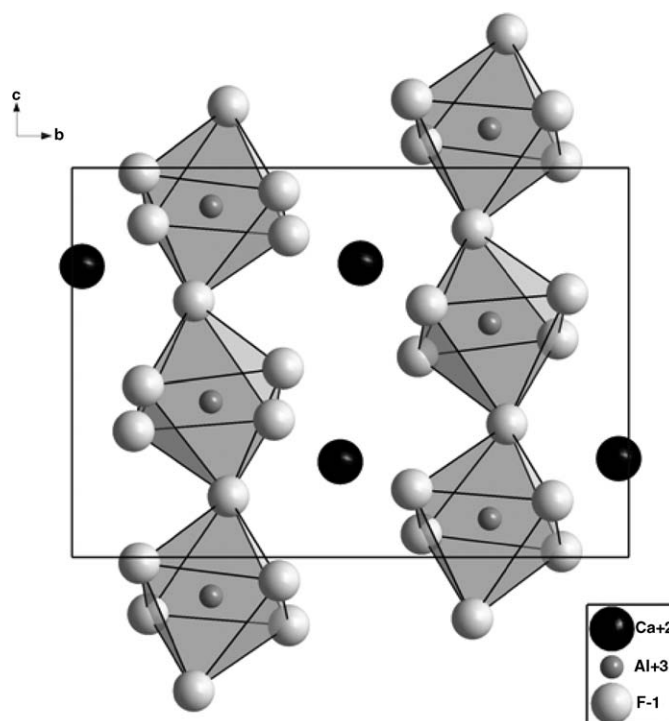

Fig. 2. Projection in $(\vec{b}, \vec{c})$ plane of β-CaAlF$_5$ structure.

155.8°, in between the values evaluated at 150.5° and 157.5° respectively for CaFeF$_5$ [6], and α-CaAlF$_5$ [18]. The Ca atoms are located between four chains of AlF$_6^{3-}$ octahedra and are surrounded by seven fluorine atoms that form pentagonal bi-pyramids. These CaF$_7^{5-}$ polyhedra form edge-sharing chains that are running also along the c axis.

If the mean Al–F distance (1.793 Å) is usual, the shortest Al–F distance (1.689 Å) is quite small and the longest one (1.907 Å) is quite large. Nevertheless, such Al–F distances have been already encountered in γ-CsAlF$_4$ (1.654, 1.962 and 1.988 Å) [19], and in β-Ba$_3$AlF$_9$ (1.678, 1.682 and 1.966 Å) [20]. Note that these two structures are also powder-refined structures. The Ca–F distances are between 2.217 and 2.558 Å, and are similar to those found in α-CaAlF$_5$ [18], Ca$_2$AlF$_7$ [21] and CaFeF$_5$ [6]. The angular distortions of the AlF$_6^{3-}$ octahedra are also quite important. The F–Al–F angles (Table 2) are ranging from 165.0° to 177.7°, and from 84.2° to 97.9° respectively for 180.0°, and 90.0° values expected in a regular octahedron. However, these values are not very different from those of the FeF$_6^{3-}$ octahedra in CaFeF$_5$ [6] ranging between 165.7° and 178.0°, and 81.7° and 97.9° respectively. Moreover, within the MAlF$_5$ compounds, isotypic β-SrAlF$_5$ [22] and EuAlF$_5$ [23] built up from dimer Al$_2$F$_{10}^{4-}$ units, present even more distorted octahedra, with angles ranging from 75.3° to 106.3°, and from 164.4° to 179.5°.

Thus, starting from the CaFeF$_5$ atomic positions given in [5] for the refinement, we obtained a solution for which the anomalies reported for the starting solution are removed (less distorted AlF$_6^{3-}$ octahedra and CaF$_7^{5-}$ pentagonal bipyramids are found) in agreement with the recent CaFeF$_5$ structure redetermination [6].

Comparing Al–F bond distances and F–Al–F bond angles in α [18] and β-CaAlF$_5$, the AlF$_6^{3-}$ octahedra appear to be more distorted in the β phase. This is in agreement with the lower symmetry of the β phase, which is related to five different fluorine sites instead of three in α-CaAlF$_5$.

3.3. ^{19}F NMR

The ^{19}F NMR spectrum of β-CaAlF$_5$ was previously recorded at 282.3 MHz (Fig. 11 of [7]). Four lines were resolved and from their positions and relative intensities, we found 20% of shared (bridging two octahedra) and 80% of unshared fluorine atoms, which indicates that β-CaAlF$_5$ is built up from isolated chains of AlF$_6^{3-}$ octahedra [7]. This is in agreement with the structure.

In order to improve the resolution, ^{19}F NMR spectra of β-CaAlF$_5$ were recorded at 705.7 MHz. Fig. 3 gives evidence for five lines clearly resolved in the spectrum. Moreover, the reconstructions of the experimental spectra at various spinning speeds lead to five contributions of equal intensity. This is consistent with five fluorine sites with the same multiplicity. Line labels, intensities, and experimental isotropic chemical shifts issued from the
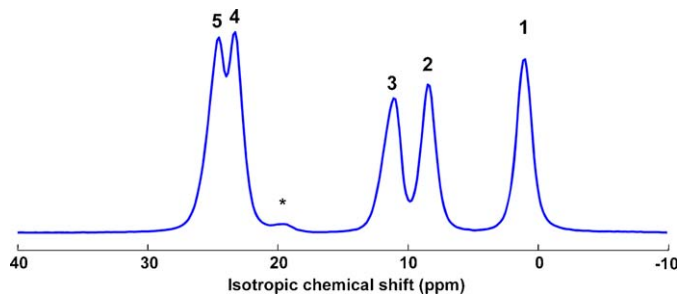

Fig. 3. ^{19}F MAS NMR spectra of β-CaAlF$_5$ collected at 17 T for $v_r = 34$ kHz. The symbol * indicates a non-identified impurity.

Table 3
Line labels, relative intensities (%) and δ$_{iso,exp}$ values (ppm) as deduced from NMR ^{19}F MAS spectrum simulations, δ$_{iso,cal}$ with the superposition model, Δδ$_{iso}$ = δ$_{iso,exp}$–δ$_{iso,cal}$ and line attributions

Line	Relative intensity (±2%)	δ$_{iso,exp}$ (±1 ppm)	δ$_{iso,cal}$ (±0.1 ppm)	Δδ$_{iso}$	Site
1	18	2	2.0	0.0	**F4(s)**
2	20	9	12.0	−3.0	**F1(u)**
3	19	12	18.4	−6.4	F2(u)
4	19	24	23.1	0.9	**F3(u)**
5	23	25	36.2	−11.2	F5(u)

s and u indicate respectively shared and unshared fluorine atoms. Unambiguous attributions are in boldface.

simulation of the spectrum recorded at 34 kHz are gathered in Table 3.

3.4. ^{27}Al NMR

Previously, ^{27}Al MAS NMR spectra of β-CaAlF$_5$ were recorded by Sakida et al. [24]. However they were not able to determine the isotropic chemical shift and quadrupolar parameter values, due to the poor quality of the spectra.

In contrast our ^{27}Al SATRAS NMR spectrum (Fig. 4) presents a central transition with a specific line shape (Fig. 4 inset) and satellite transitions symmetrically expanded over 1.5 MHz. Such a large expansion is related to a very large value of the quadrupolar frequency. The reconstruction of the whole spectrum allows a precise determination of the quadrupolar parameters. The NMR parameters leading to the best simulation are: δ$_{iso}$ = −7(±1) ppm, v_Q = 1.53(±0.08) MHz, and η$_Q$ = 0.10(±0.05). The first two extra lines that appear on both sides of the central transition are reconstructed taking into account the asymmetry of the chemical shift with: δ$_{aniso}$ = −300 (±50) ppm, and 0 < η < 0.30. The reconstructed spectrum is compared with the experimental one in Fig. 4. The isotropic chemical shift value is typical of an Al^{3+} ion surrounded by six fluorine atoms and the η$_Q$ value which is different from zero indicates the AlF$_6^{3-}$ octahedra are rhombically distorted. These results support the determined structure.
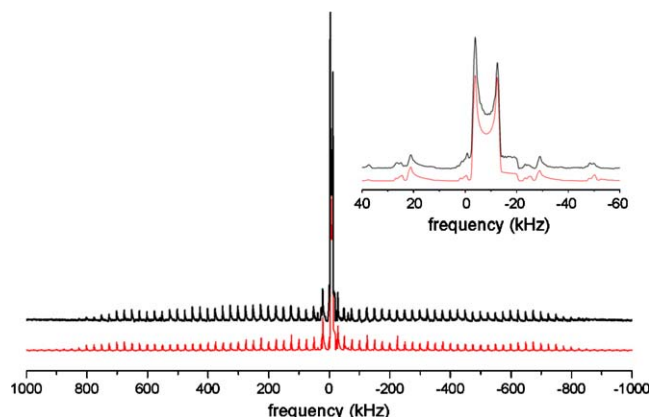
Fig. 4. Experimental (up) and reconstructed (down) ^{27}Al SATRAS NMR spectra of β-CaAlF$_5$ at 25 kHz. The central transition is presented in the inset.

Table 4
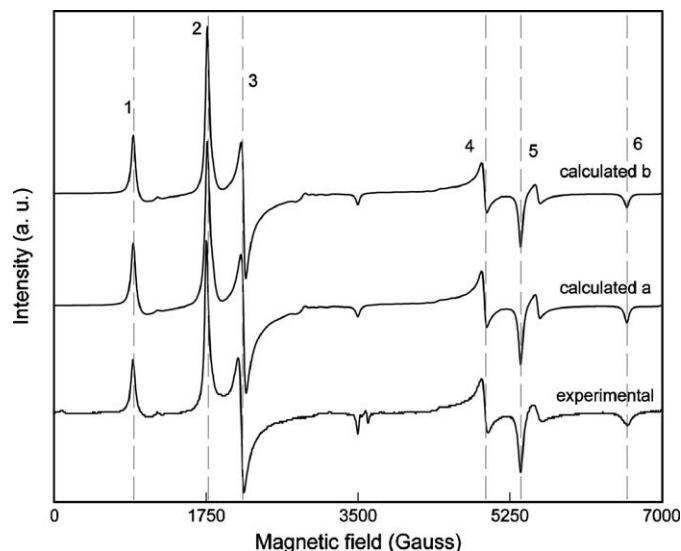Experimental and calculated ^{27}Al NMR quadrupolar and Cr^{3+} EPR fine structure parameters for β-CaAlF$_5$

	ν_Q (MHz)	η_Q	b_2^0 (10^{-4} cm^{-1})	λ
Experimental	1.53 (± 0.08)	0.10 (± 0.05)	2455 (± 20)	0.19 (± 0.01)
Calculated	1.84	0.18	2431	0.64
	1.38	*0.09*	*2527*	*0.42*

The values in italic are obtained using the WIEN2k optimized structural data.

intensity is too high and the line 6 is too narrow. A slightly better reconstruction is obtained with small b_2^m distribution (spectrum *b*); line 1 intensity is still, but less, too high and the lines 4 and 5 intensities are too small. Broader b_2^m distributions reduce the agreement between the observed and reconstructed spectra. Such a narrow distribution demonstrates the good crystalline quality of our sample.

A similar spectrum with an additional very intense central line was previously reported in [25] as the spectrum of Cr^{3+} in α-CaAlF$_5$. However, there is no doubt that this studied phase was β-CaAlF$_5$ due to the value of heating temperature (850 °C) and the quenching step used in the synthesis process. The very intense central line cannot be attributed to Cr^{3+} in β-CaAlF$_5$. Furthermore, the fine structure parameter values given in [25] ($D(= b_2^0) = 1415$ G; $E(= b_2^2/3) = 66.5$ G, that is to say $b_2^0 = 1308 \times 10^{-4}$ cm^{-1} and $b_2^2 = 184 \times 10^{-4}$ cm^{-1}) appear to be incorrect as they do not allow any reliable reconstruction of the experimental spectrum.

4. Spectroscopic parameter modelling and discussion

4.1. ^{19}F NMR isotropic chemical shift

The superposition model [10] as refined in [7] was used for the calculation of the isotropic chemical shift from the crystallographic data. In [7], the Root Mean Square (RMS) deviation was found equal to 6 ppm, and only cations included in a sphere of 3.5 Å radius were considered since for larger distances the cationic contributions become negligible. The calculated and experimental isotropic chemical shifts were then paired in order to minimize the difference:

$$\Delta\delta_{iso} = \delta_{iso,exp} - \delta_{iso,cal}.$$

The values obtained with this model are gathered with the experimental results in Table 3. So, attribution of F4 to line 1, F1 to line 2 and F3 to line 4 is certain, as the difference between their calculated and experimental δ_{iso} values is small, within the RMS deviation of 6 ppm. The attribution of line 1 ($\delta_{iso} = 2$ ppm) to the shared fluorine atom, and, consequently the attribution of lines 2 to 5 to unshared ones are in agreement with the chemical shift

Fig. 5. Experimental and reconstructed EPR spectra of β-CaAlF$_5$: Cr^{3+}. $g_x = g_y = 1.96$ (± 0.01), $g_z = 1.975$ (± 0.01), $b_2^0 = 2455$ (± 20) $\times 10^{-4}$ cm^{-1}, and $b_2^2 = 460$ (± 20) $\times 10^{-4}$ cm^{-1}. (a) $\Gamma_0 = 60$ (± 5) G, $\delta b_2^0 = 0$ and $\delta b_2^2 = 0$. (b) $\Gamma_0 = 50$ (± 5) G, $\delta b_2^0 = \delta b_2^2 = 10$ (± 10) $\times 10^{-4}$ cm^{-1}.

3.5. EPR study of β-CaAlF$_5$:Cr^{3+} powder

The observed spectrum, previously reported in [16], the calculated spectra and the spin-Hamiltonian parameters leading to the best agreement are gathered in Fig. 5. The b_2^2 and λ values (Table 4) are different from zero, which is consistent with rhombically distorted AlF$_6^{3-}$ octahedra.

In Fig. 5, experimental spectrum and reconstructed spectra have all the same intensity (scaled on lines 2 and 3). A fine agreement between the observed spectrum and the reconstructed ones with respect to line positions is obtained. For the reconstructed spectrum *a*, without distribution of b_2^m parameters, the agreement is also good for lines relative intensity. Nevertheless, if one looks carefully at the spectra, one can note that the line 1

ranges previously defined for shared and unshared fluorine atoms in the CaF_2–AlF_3 binary system [7].

4.2. ^{27}Al NMR quadrupolar parameters

The Electric Field Gradient (EFG) tensor characterizes the distribution of the electronic charge surrounding a nucleus with a nuclear quantum number $I > 1/2$. The quadrupolar frequency v_Q and the asymmetry parameter η_Q can be related to the components of the EFG tensor, through the following equations:

$$v_Q = \frac{3eQV_{zz}}{2I(2I-1)h} \quad \text{and} \quad \eta_Q = \frac{V_{xx} - V_{yy}}{V_{zz}}.$$

Ab-initio calculation of EFG were performed using the Wien2k code [26] which is a full potential (linearized) augmented plane wave code for periodic systems.[1] The crystalline structure issued from the Rietveld refinement was used for this calculation. Sphere sizes of 1.54, 1.55 and 1.80 a.u. for F, Al and Ca respectively were used and the basis set was determined by a large cutoff corresponding to $RK_{max} = 8$ (about 5800 plane waves). The full Brillouin zone (BZ) was sampled with 100 k-points and we used the generalized gradient approximation (GGA) of Perdew et al. [27] for the description of exchange and correlation effects within density functional theory. First the structure was optimized by adjusting the atomic positions of β-$CaAlF_5$, keeping the experimental cell parameters unchanged, until the forces acting on all atoms (with a maximum of 59 mRy/a.u. for the F5 atom) were reduced to below 2 mRy/a.u. The experimental powder XRD pattern and the calculated one from the optimized structure are superimposed in Fig. 6. The two calculated patterns shown in Figs. 1 and 6 can be hardly distinguished, which is confirmed by the closeness of both the difference patterns, and the R_P factors equal to 0.106 and 0.132 respectively. The positional parameters, selected bond distances and angles for the optimized structure of β-$CaAlF_5$ are given in Tables 1 and 2 respectively. Comparison with the crystallographic data shows that the mean Al–F distance is slightly increased to 1.820 Å when the mean Ca–F one is decreased. The main point to outline is that the radial and angular distortions of the AlF_6^{3-} octahedron are significantly reduced.

The values of V_{zz} calculated from the experimental and optimized structures are found equal to 3.49×10^{21} and 2.61×10^{21} V/m^2 respectively. The corresponding quadrupolar frequencies are deduced using the most recently determined nuclear quadrupole moment Q $(^{27}Al) = 1.460 \times 10^{-29}$ m^2 [28]. The calculated quadrupolar parameters are given in Table 4. A remarkable agreement with the experimental values is obtained after optimization. This agreement concerns not only the quadrupolar frequency
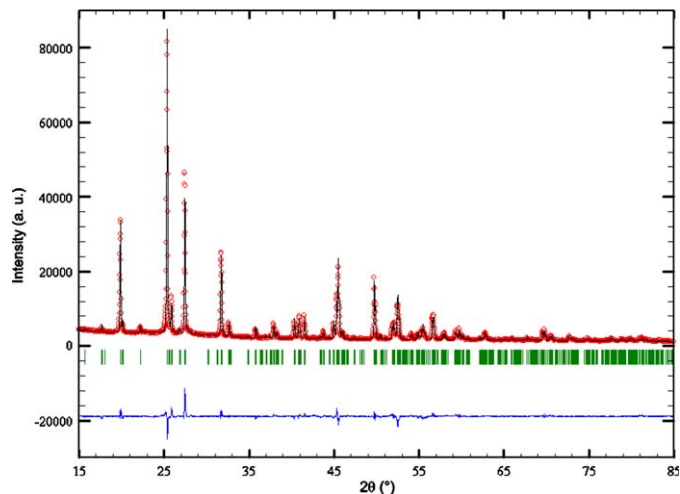
Fig. 6. Observed (points) and calculated from WIEN2k optimized structural data (line) powder X-ray diffraction patterns of β-$CaAlF_5$. The difference pattern is shown below at the same scale, the vertical bars are related to the calculated Bragg reflection positions.

but also the asymmetry parameter which is much more difficult to reproduce [29]. This may be related to its high sensitivity to variations of the atomic positions around the studied nucleus.

Finally, it is interesting to note that NMR is much more sensitive to the geometry than powder XRD. Indeed, the NMR parameters obtained with the two structures are clearly different (Table 4) whereas the calculated powder diffraction patterns (Figs. 1 and 6) are practically identical.

4.3. Cr^{3+} EPR fine structure parameters

The superposition model of Newman [30] assumes that the spin Hamiltonian parameters depend on the local surrounding of the paramagnetic ion through the law:

$$b_n^m = \sum_i b_n(R_i) K_n^m(\theta_i, \varphi_i),$$

where i runs over the nearest neighbours at polar coordinates R_i, θ_i and φ_i. The $K_n^m(\theta_i, \varphi_i)$ are spherical harmonics functions of rank n of the polar angles. The $b_n(R_i)$ are functions of the radial metal ligand distances R_i. They depend on the probe and ligand type. From several experimental results on fluoroaluminate crystallized compounds, Houlbert [31] determined $b_2(R)$ function for Cr^{3+} (figure is given in [32]). It can be expressed as

$$b_2(R) = \left\{ 16000 + (R(\text{Å}) - 1.9\,\text{Å}) \frac{1000}{(1.9 - 1.808)\,\text{Å}} \right\} \times 10^{-4}\,\text{cm}^{-1}$$
$$\text{for } 1.65\,\text{Å} \leqslant R(\text{Å}) \leqslant 1.95\,\text{Å}.$$

This function was previously applied in [32–34].

b_2^m values are calculated under the assumption that the substitution is achieved without any lattice relaxation. The values of the fine structure parameters b_2^0 and λ calculated

from the refined and optimized structures, and expressed in the principal axis system of the interaction, are given in Table 4. The b_2^0 values are very close to the experimental one. The agreement is not so fine for the λ values which may be related to some structural relaxation around the Cr^{3+} ions. Nevertheless, the atomic positions of the optimized structure lead to the smallest discrepancy.

5. Conclusion

The precise structure of β-CaAlF$_5$, isotypic with CaFeF$_5$, is determined for the first time. The experimental results using local probe spectroscopies confirm this structure. The five lines of the high speed ^{19}F MAS NMR spectra are in agreement with the five fluorine sites. Their chemical shifts are also consistent with a structure built-up from infinite isolated chains of AlF_6^{3-} octahedra: 20% of the fluorine atoms are shared and 80% unshared. ^{27}Al SATRAS NMR and Cr^{3+} EPR spectra indicate one aluminium site and the experimental δ_{iso} (^{27}Al) value is typical of AlF_6^{3-} octahedra. The η_Q and λ asymmetry parameter values issued from the reconstruction are both different from zero, in agreement with rhombically distorted AlF_6^{3-} octahedra.

Using the refined structure and the superposition model developed for the fluorine isotropic chemical shift [7,10], it was possible to attribute fluorine sites F4, F1 and F3 to the NMR lines 1, 2 and 4 respectively.

As generally done (see for instance [35,36]), it was necessary to optimize the structure to improve the agreement between calculated and experimental quadrupolar parameters. The structure of β-CaAlF$_5$ was then optimized using WIEN2k code [26] which leads to calculated v_Q and η_Q values remarkably close to the experimental ones.

Calculation of the fine structure parameters using the superposition model of Newman [30] leads to a good agreement between experimental and calculated values for b_2^0. It is not so satisfactory for λ certainly due to the structure relaxation around the Cr^{3+} ion.

Modelling of the experimental spectroscopic parameters supports the reliability of the determined structure. This work illustrates an interesting example of a powder XRD structure determination complemented with magnetic resonance (NMR and EPR) investigations and theoretical predictive calculations of spectroscopic parameters using empirical and ab-initio methods.

Acknowledgments

References

[1] D. Craig, J. Brown, J. Am. Ceram. Soc. 60 (1977) 396–398.

[2] J.P. Millet, M. Rolin, M. Rev. Int. Hautes Tempér. Refract. 18 (1981) 287–292.

[3] J.L. Holm, Acta Chem. Scand. 19 (1965) 1512–1514.

[4] J. Ravez, P. Hagenmuller, Bull. Soc. Chim. Fr. 7 (1967) 2545–2548.

[5] R. Von der Mühll, J. Ravez, Rev. Chimie Min. 11 (1974) 652–663.

[6] J. Graulich, W. Massa, D. Babel, Z. Anorg. Allg. Chem. 629 (2003) 365–367.

[7] M. Body, G. Silly, C. Legein, J.-Y. Buzaré, Inorg. Chem. 43 (2004) 2474–2485.

[8] H.M. Rietveld, J. Appl. Crystallogr. 2 (1969) 65–71.

[9] J.R. Carjaval, FULLPROF Program, Rietveld Pattern Matching Analysis of Powder Patterns, ILL, Grenoble, 1990.

[10] B. Bureau, G. Silly, J. Emery, J.-Y. Buzaré, Chem. Phys. 249 (1999) 89–104.

[11] D. Massiot, F. Fayon, M. Capron, I. King, S. Le Calvé, B. Alonso, J.-O. Durand, B. Bujoli, Z. Gan, G. Hoatson, Magn. Reson. Chem. 40 (2002) 70–76.

[12] J. Skibsted, N.C. Nielsen, H.J. Bildsoe, H.J. Jakobsen, J. Magn. Reson. 95 (1991) 88–117.

[13] J. Skibsted, N.C. Nielsen, H. Bildsoe, H.J. Jakobsen, Chem. Phys. Lett. 188 (1992) 405–412.

[14] S. Ding, C.A. McDowell, Chem. Phys. Lett. 333 (2001) 413–418.

[15] G. Scholz, R. Stösser, J. Klein, J.-Y. Buzaré, G. Silly, Y. Laligant, B. Ziemer, J. Phys.: Condens. Matter. 14 (2002) 2101–2117.

[16] J.-Y. Buzaré, C. Legein, G. Silly, J. Émery, OHD Proc. (Le Mans) (2001) 37–40.

[17] J.-Y. Buzaré, G. Silly, J. Klein, G. Scholz, R. Stösser, M. Nofz, J. Phys.: Condens. Matter. 14 (2002) 10331–10348.

[18] A. Hémon, G. Courbion, Acta. Cryst. C 47 (1991) 1302–1303.

[19] U. Bentrup, A. Le Bail, H. Duroy, J.-L. Fourquet, Eur. J. Solid State Inorg. Chem. 29 (1992) 371–381.

[20] A. Le Bail, J. Solid State Chem. 103 (1993) 287–291.

[21] R. Domesle, R. Hoppe, Z. Kristallogr. 153 (1980) 317–328.

[22] F. Kubel, Z. Anorg. Allg. Chem. 624 (1998) 1481–1486.

[23] M. Weil, F. Kubel, J. Solid State Chem. 164 (2002) 150–156.

[24] S. Sakida, M. Shojiya, Y. Kawamoto, J. Fluorine Chem. 106 (2000) 127–131.

[25] J.-M. Dance, J.-J. Videau, J. Portier, J. Non-Cryst. Solids 86 (1986) 88–93.

[26] P. Blaha, K. Schwarz, G.K.H. Madsen, D. Kvasnicka, J. Luitz, WIEN2k, An Augmented Plane Wave plus Local Orbitals Program for Calculating Crystal Properties, Vienna University of Technology, Austria, ISBN 3-9501031-1-2, 2001.

[27] J.P. Perdew, K. Burke, M. Ernzerhof, Phys. Rev. Lett. 77 (1996) 3865–3868.

[28] P. Pyykkö, Mol. Phys. 99 (2001) 1617–1629.

[29] P.L. Bryant, C.R. Harvell, K. Wu, F.R. Fronczek, R.W. Hall, L.G. Butler, J. Phys. Chem. A 103 (1999) 5246–5252.

[30] D.J. Newman, Adv. Phys. 20 (1971) 197–256.

[31] S. Houlbert, Thesis, University of Caen, France, 1992.

[32] C. Legein, J.-Y. Buzaré, B. Boulard, C. Jacoboni, J. Phys.: Condens. Matter. 7 (1995) 4829–4846.

[33] G. Scholz, R. Stösser, C. Legein, J.-Y. Buzaré, G. Silly, Appl. Magn. Res. 18 (2000) 199–215.

[34] C. Legein, J.-Y. Buzaré, C. Jacoboni, J. Solid State Chem. 121 (1996) 149–157.

[35] M. Iglesias, K. Schwarz, P. Blaha, D. Baldomir, Phys. Chem. Miner. 28 (2001) 67–75.

[36] B. Zhou, T. Giavani, H. Bildsoe, J. Skibsted, H.J. Jakobsen, Chem. Phys. Lett. 402 (2005) 133–137.